Multiatom entanglement dynamics and entanglement transfer between remote cavities via optical fibers

Qi-Liang He, Ye-Qi Zhang, and Jing-Bo Xu

Abstract: We investigate the entanglement dynamics of a system that consists of four single-mode cavities that are spatially separated and connected by two optical fibers, with multiple two-level atoms trapped in each cavity. It is shown that the phenomenon of entanglement sudden death and sudden birth appears in this system and is sensitive to the initial conditions and the parameter *r*. In addition, we also study the entanglement and entangled state transfer between the atoms and find that a perfect transfer can be realized if the value of the parameter *r* satisfies a certain condition, established here.

PACS Nos: 03.65.Ud, 03.67.Mn, 03.67.Hk

Résumé : Nous étudions la dynamique d'intrication d'un système constitué de quatre cavités unimodales spatialement séparées et reliées par deux fibres optiques, avec plusieurs atomes à deux niveaux piégés dans chaque cavité. Nous montrons que la disparition soudaine et l'émergence soudaine de l'intrication sont toutes deux possibles dans ce système et leur apparition dépend des conditions initiales et du paramètre *r*. De plus, nous étudions aussi l'intrication et le transfert d'état intriqué entre les atomes et trouvons qu'un transfert parfait peut être réalisé si la valeur du paramètre *r* satisfait les conditions établies.

[Traduit par la Rédaction]

1. Introduction

Quantum entanglement was first introduced by Einstein, Podolsky, and Rosen (EPR) in their famous paper, published in 1935 [1]. It is a special quantum correlation and plays a key role in quantum information processing [2–5]. A fundamental feature of entanglement is that it is easily degraded when the entangled system interacts with another system or environment [6–11]. It is pointed out by Yu and Eberly [6, 11] that the entanglement between two qubits interacting with uncorrelated reservoirs may disappear within a finite time during the dynamics evolution. This phenomenon, called entanglement sudden death (ESD), has been observed in the lab for entangled photon pairs [12] and atomic ensembles [13]. Recently, the quantum dynamics of a system consisting of two cavities interacting with two independent reservoirs has been studied [14]. It is shown that ESD in a bipartite system independently coupled to reservoirs is related to the entanglement sudden birth (ESB) [9, 10] and that the ESB could occur after, simultaneously with, or even before ESD.

On the other hand, the possibility of quantum information processing realized via optical fibers has also attracted much attention [15–18]. Generating and transferring the entangled state of distant qubits has been recognized as a key element of quantum computation and teleportation. Bose et al. propose a scheme to realize the effective quantum gates between two atoms in distant cavities coupled by optical fibers [19]. The protocol for realizing the transfer of quantum information on such a system has also been studied [20].

In this paper, we investigate multiatom entanglement dynamics, entanglement, and entangled state transfer of a system consisting of two identical subsystems (see Fig. 1). Each subsystem contains multiple two-level atoms that are trapped in two distant single-mode optical cavities, which are connected by two optical fibers. It is shown that the phenomena of ESD and ESB may appear in this system and that the amount of entanglement of the atoms, or the other bipartite partitions of the system, depends on the initial state and the parameter *r*. Moreover, we also study the entanglement and entangled state transfer between the atoms. It is not difficult to see that a perfect entanglement and entangled state transfer can be achieved if we choose the appropriate value of the parameter *r*.

The present paper is organized as follows. In Sect. 2, we introduce the model under consideration and the entanglement dynamics. In Sect. 3, we use concurrence to study the ESD and ESB in this quantum system. In Sect. 4, we investigate the entanglement and the entangled state transfer between the atoms. The final section is a summary.

Received 17 December 2010. Accepted 22 April 2011. Published at www.nrcresearchpress.com/cjp on 26 July 2011.

Q.-L. He, Y.-Q. Zhang, and J.-B. Xu. Zhejiang Institute of Modern Physics and Physics Department, Zhejiang University, Hangzhou 310027, People's Republic of China.

Corresponding author: Jing-Bo Xu (e-mail: xujb@zju.edu.cn).

Fig. 1. This is the schematic diagram of the system investigated in the present paper.

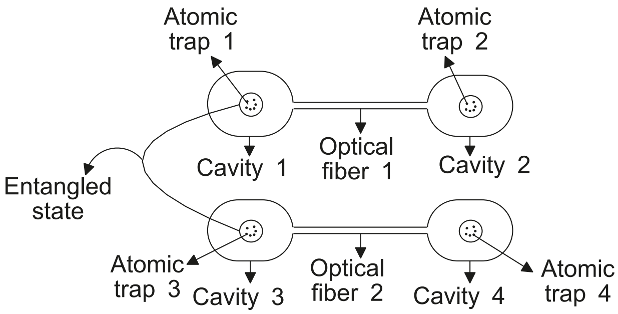

2. The model and its solution

As shown in Fig. 1, we consider the system to be composed of two identical subsystems [18]. Each subsystem contains multiple two-level atoms that are trapped in two distant single-mode optical cavities, and the cavities are connected by two optical fibers. Here, we assume that the evolution of each subsystem is independent and that the atoms in the same cavity are separated enough that they have no direct interaction with one another. In the short fiber limit [18], only one resonant mode of the fiber interacts with the interrelated cavity-mode. Therefore, for this case, the Hamiltonian of the whole system can be written as ($\hbar = 1$)

$$H = \sum_{j=1}^{4}\left(\omega a_j^\dagger a_j + \omega_a J_j^z\right) + \sum_{j=1}^{2}\omega\left(b_j^\dagger b_j\right) + \sum_{j=1}^{4}\left(g_j J_j^- a_j^\dagger + \text{H.c.}\right) + \nu_1\left[b_1\left(a_1^\dagger + a_2^\dagger\right) + \text{H.c.}\right] + \nu_2\left[b_2\left(a_3^\dagger + a_4^\dagger\right) + \text{H.c.}\right] \quad (1)$$

where $a_j^\dagger$ (a_j) and $b_j^\dagger$ (b_j) are the creation and annihilation operators of the jth cavity field and the jth fiber mode of frequency ω, respectively; g_j is the coupling constant between the mode of cavity j and the trapped atoms; ν_j is the coupling strength of the jth fiber mode and its neighbor cavities; H.c. denotes the Hermitian conjugate; $J_j^z = \sum_{i=1}^{N_j}\sigma_i^z(j)$ with $\sigma_i^z(j) = (|e_i\rangle\langle e_i| - |g_i\rangle\langle g_i|)/2$ for atom i in cavity j; $J_j^\dagger$ and J_j^- are the collectively raising and lowering operators for the atoms in cavity j (j = 1, 2, 3, 4) which are defined as

$$J_j^{\pm} = \sum_{i=1}^{N_j}\sigma_i^{\pm}(j) \quad (2)$$

where N_j is the number of atoms in cavity j, $\sigma_i^-(j) = |g_i\rangle\langle e_i|$ and $\sigma_i^\dagger(j) = |e_i\rangle\langle g_i|$ are the atomic spin flip operators for atom i in cavity j, and $|g\rangle$ and $|e\rangle$ are the ground and excited states of the atom, respectively. Here, we consider that the interaction between the atoms and the cavity fields is on resonance ($\omega_a = \omega$). For simplicity, we set $\nu_1 = \nu_2 = \nu$, all the atom–field coupling constants are equal, and the number of atoms in each cavity remains the same throughout this paper.

We now investigate the dynamics of entanglement in this system. First, we assume that the initial state of the whole system at $t = 0$ is prepared in

$$|\Psi(0)\rangle = (\alpha|1, N-1\rangle_1|1, N-1\rangle_3 + \beta|0, N\rangle_1|0, N\rangle_3) \otimes |0, N\rangle_2 \otimes |0, N\rangle_4 \otimes |000\rangle_{c_1c_2f_1} \otimes |000\rangle_{c_3c_4f_2} \quad (3)$$

where, α and β are complex numbers with the condition $|\alpha|^2 + |\beta|^2 = 1$.

In (3), the state $|0, N\rangle$ represents that N atoms are all in the ground state of the computational basis $|0\rangle$. Similarly, the $|1, N-1\rangle$ represents that $N - 1$ atoms are in the ground state and one atom is in the excited state of the computational basis $|1\rangle$.

In the interaction picture, it is not difficult to find that the state of the whole system at time t is

$$|\psi(t)\rangle = \alpha[A_1(t)|\phi_1\rangle + B_1(t)|\phi_2\rangle + C_1(t)|\phi_3\rangle + D_1(t)|\phi_4\rangle + E_1(t)|\phi_5\rangle] \otimes [A_1(t)|\phi_6\rangle + B_1(t)|\phi_7\rangle + C_1(t)|\phi_8\rangle + D_1(t)|\phi_9\rangle + E_1(t)\phi_{10}\rangle] + \beta[|0, N\rangle_1|0, N\rangle_2|000\rangle_{c_1c_2f_1}|0, N\rangle_3|0, N\rangle_4|000\rangle_{c_3c_4f_2}] \quad (4)$$

with

$$A_1(t) = \frac{r^2}{1+2r^2} - \frac{1}{2}\cos\left(\sqrt{N}gt\right) + \frac{\cos\left(\sqrt{1+2r^2}\sqrt{N}gt\right)}{2\left(1+2r^2\right)}$$

$$B_1(t) = \frac{r^2}{1+2r^2} + \frac{1}{2}\cos\left(\sqrt{N}gt\right) + \frac{\cos\left(\sqrt{1+2r^2}\sqrt{N}gt\right)}{2\left(1+2r^2\right)}$$

$$C_1(t) = -\frac{i}{2}\sin\left(\sqrt{N}gt\right) + \frac{i\sin\left(\sqrt{1+2r^2}\sqrt{N}gt\right)}{2\left(1+2r^2\right)}$$

$$D_1(t) = -\frac{r}{1+2r^2} + \frac{r\cos\left(\sqrt{1+2r^2}\sqrt{N}gt\right)}{1+2r^2}$$

$$E_1(t) = \frac{i}{2}\sin\left(\sqrt{N}gt\right) + \frac{i\sin\left(\sqrt{1+2r^2}\sqrt{N}gt\right)}{2\left(1+2r^2\right)}$$

$$r = \frac{\nu}{\sqrt{N}g}$$

$$\begin{aligned}
|\phi_1\rangle &= |0, N\rangle_1|1, N-1\rangle_2|000\rangle_{c_1c_2f_1}\\
|\phi_2\rangle &= |1, N-1\rangle_1|0, N\rangle_2|000\rangle_{c_1c_2f_1}\\
|\phi_3\rangle &= |0, N\rangle_1|0, N\rangle_2|010\rangle_{c_1c_2f_1}\\
|\phi_4\rangle &= |0, N\rangle_1|0, N\rangle_2|001\rangle_{c_1c_2f_1}\\
|\phi_5\rangle &= |0, N\rangle_1|0, N\rangle_2|100\rangle_{c_1c_{2_2}f_1}\\
|\phi_6\rangle &= |0, N\rangle_3|1, N-1\rangle_4|000\rangle_{c_3c_4f_2}\\
|\phi_7\rangle &= |1, N-1\rangle_3|0, N\rangle_4|000\rangle_{c_3c_4f_2}\\
|\phi_8\rangle &= |0, N\rangle_3|0, N\rangle_4|010\rangle_{c_3c_4f_2}\\
|\phi_9\rangle &= |0, N\rangle_3|0, N\rangle_4|001\rangle_{c_3c_4f_2}\\
|\phi_{10}\rangle &= |0, N\rangle_3|0, N\rangle_4|100\rangle_{c_3c_4f_2}
\end{aligned} \quad (5)$$

3. Entanglement sudden death and sudden birth

In this section, we investigate the phenomena of ESD and ESB in this system. To quantify the degree of entanglement, we use the concurrence introduced by Wotters [21]. For a two-qubit system, the concurrence can be defined as

$$C(\rho) = \max\left\{0, \sqrt{\lambda_1} - \sqrt{\lambda_2} - \sqrt{\lambda_3} - \sqrt{\lambda_4}\right\} \tag{6}$$

where λ_i ($i = 1, 2, 3, 4$) are the eigenvalues in decreasing order of the magnitude of the "spin-flipped" density matrix operator $R = \rho(\sigma_y \otimes \sigma_y)\rho^* (\sigma_y \otimes \sigma_y)$, where σ_y is the Pauli Y matrix, and ρ^* is the complex conjugate of ρ. Particularly, if the density matrix, ρ, can be written in the form of X-states

$$\rho = \begin{pmatrix} a & 0 & 0 & f \\ 0 & b & e & 0 \\ 0 & e^* & c & 0 \\ f^* & 0 & 0 & d \end{pmatrix} \tag{7}$$

where $a + b + c + d = 1$, the concurrence can be easily computed as [22]

$$C(\rho) = 2\max\left\{0, |e| - \sqrt{ad}, |f| - \sqrt{bc}\right\} \tag{8}$$

Tracing over the other degrees of this system, we obtain the reduced density matrix of atomic traps 1 and 3

$$\begin{aligned}\rho_{13}(t) = {} & a(t)|1, N-1\rangle|1, N-1\rangle\langle 1, N-1|\langle 1, N-1| \\ & + b(t)|1, N-1\rangle|0, N\rangle\langle 1, N-1|\langle 0, N| \\ & + c(t)|0, N\rangle|1, N-1\rangle\langle 0, N|\langle 1, N-1| \\ & + d(t)|0, N\rangle|0, N\rangle\langle 0, N|\langle 0, N| \\ & + f(t)|1, N-1\rangle|1, N-1\rangle\langle 0, N|\langle 0, N| \\ & + f^*(t)|0, N\rangle|0, N\rangle\langle 1, N-1|\langle 1, N-1|\end{aligned} \tag{9}$$

with

$$\begin{aligned} a(t) &= |\alpha|^2|B_1^2(t)|^2 \\ b(t) &= c(t) = |\alpha|^2|A_1(t)B_1(t)|^2 + |\alpha|^2|B_1(t)C_1(t)|^2 \\ &\quad + |\alpha|^2|B_1(t)D_1(t)|^2 + |\alpha|^2|B_1(t)E_1(t)|^2 \\ d(t) &= |\alpha|^2|A_1^2(t)|^2 + |\alpha|^2|C_1^2(t)|^2 + |\alpha|^2|D_1^2(t)|^2 \\ &\quad + |\alpha|^2|E_1^2(t)|^2 + 2|\alpha|^2|A_1(t)C_1(t)|^2 + 2|\alpha|^2|A_1(t)D_1(t)|^2 \\ &\quad + 2|\alpha|^2 + 2|\alpha|^2|A_1(t)E_1(t)|^2 + 2|\alpha|^2|C_1(t)D_1(t)|^2 \\ &\quad + 2|\alpha|^2|C_1(t)E_1(t)|^2 + 2|\alpha|^2|D_1(t)E_1(t)|^2 + |\beta|^2 \\ f(t) &= \alpha\beta^* B_1^2(t) \end{aligned} \tag{10}$$

Combining (8) with the reduced density matrix, we find that the concurrence of atomic traps 1 and 3 is

$$C_{13}(t) = 2\max\left\{0, |f(t)| - \sqrt{b(t)c(t)}\right\} \tag{11}$$

Similarly, the reduced density matrix of two cavities c_1 and c_3 is

$$\begin{aligned}\rho_{c_1c_3}(t) = {} & a_1(t)|00\rangle\langle 00| + b_1(t)|01\rangle\langle 01| + c_1(t)|10\rangle\langle 10| \\ & + d_1(t)|11\rangle\langle 11| + f_1(t)|00\rangle\langle 11| + f_1^*(t)|11\rangle\langle 00|\end{aligned} \tag{12}$$

Fig. 2. The concurrences, C_{13} (solid line) and $C_{c_1c_3}$ (dotted line), are plotted as a function of rescaled time, $\sqrt{N}gt$, with $|\alpha|^2 = 0.55$ and $|\beta|^2 = 0.45$. (*a*) $r = 1$; (*b*) $r = \sqrt{1.5}$.

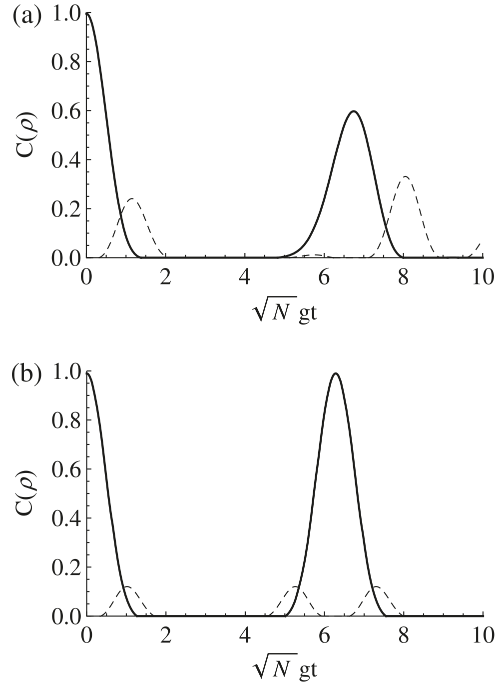

with

$$\begin{aligned} a_1(t) &= |\alpha|^2|A_1^2(t)|^2 + |\alpha|^2|B_1^2(t)|^2 + |\alpha|^2|C_1^2(t)|^2 \\ &\quad + |\alpha|^2|D_1^2(t)|^2 + 2|\alpha|^2|A_1(t)B_1(t)|^2 \\ &\quad + 2|\alpha|^2|A_1(t)C_1(t)|^2 + 2|\alpha|^2|A_1(t)D_1(t)|^2 \\ &\quad + 2|\alpha|^2|B_1(t)C_1(t)|^2 + 2|\alpha|^2|B_1(t)D_1(t)|^2 \\ &\quad + 2|\alpha|^2|C_1(t)D_1(t)|^2 + |\beta|^2 \\ b_1(t) &= c_1(t) = |\alpha|^2|A_1(t)E_1(t)|^2 + |\alpha|^2|B_1(t)E_1(t)|^2 \\ &\quad + |\alpha|^2|C_1(t)E_1(t)|^2 + |\alpha|^2|D_1(t)E_1(t)|^2 \\ d_1(t) &= |\alpha|^2|E_1^2(t)|^2 \\ f_1(t) &= \beta\alpha^* E_1^{*2}(t) \end{aligned} \tag{13}$$

and the concurrence is

$$C_{c_1c_3}(t) = 2\max\left\{0, |f_1(t)| - \sqrt{b_1(t)c_1(t)}\right\} \tag{14}$$

In Fig. 2, we plot the simultaneous concurrences, C_{13} (solid line) and $C_{c_1c_3}$ (dotted line), as a function of rescaled time, $\sqrt{N}gt$, for $|\alpha|^2 = 0.55$ and $|\beta|^2 = 0.45$ with two different values of the parameter r. From Fig. 2(*a*), we can see that the concurrence C_{13} (solid line) disappears suddenly and the concurrence $C_{c_1c_3}$ (dotted line) appears suddenly during the dynamics evolution. This means that ESD (solid line) and ESB (dotted line) may appear in this quantum system. Furthermore, the values of entanglement concurrences C_{13} and $C_{c_1c_3}$ also vary with the parameter r. After calculation, we find that the concurrence C_{13} reaches a maximum if we choose the value of parameter r to be around $\sqrt{1.5}$. The concurrence $C_{c_1c_3}$ becomes smaller when the value of parameter r increases.

Fig. 3. The concurrences, C_{13} (solid line) and $C_{c_1c_3}$ (dotted line), are plotted as a function of rescaled time, $\sqrt{N}gt$, with $r = \sqrt{1.5}$. (*a*) $|\alpha|^2 = 0.6$ and $|\beta|^2 = 0.4$; (*b*) $|\alpha|^2 = 0.8$ and $|\beta|^2 = 0.2$.

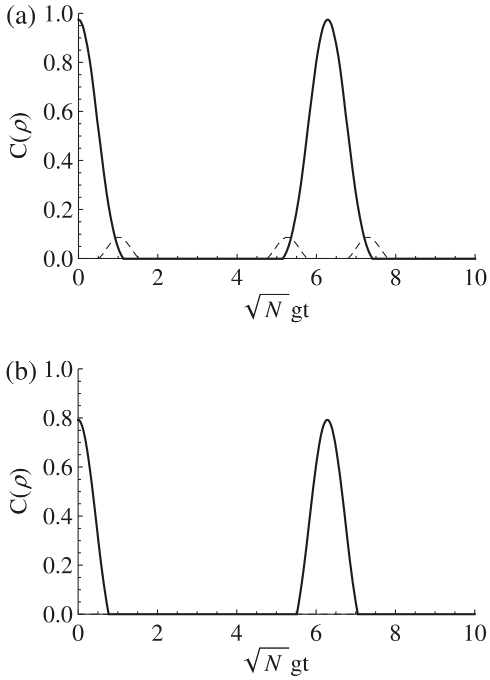

Fig. 4. The concurrence, $C_{f_1f_2}$, is plotted as a function of rescaled time, $\sqrt{N}gt$, with $|\alpha|^2 = 0.6$ and $|\beta|^2 = 0.4$. (*a*) $r = 1$; (*b*) $r = \sqrt{2}$.

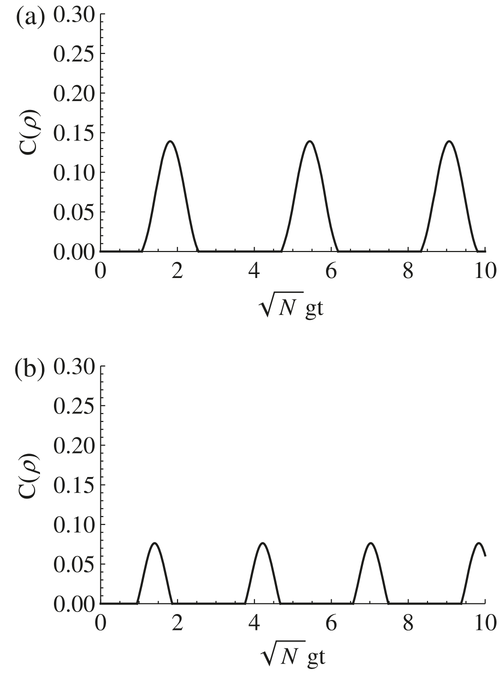

To illustrate the influence of the degree of initial entanglement on ESD and ESB, Fig. 3 illustrates the simultaneous concurrences C_{13} (solid line) and $C_{c_1c_3}$ (dotted line) as a function of rescaled time $\sqrt{N}gt$ for $r = \sqrt{1.5}$ with two different initial entanglement degrees in terms of α. It is shown that the smaller the initial degree of entanglement, the longer the state stays in the separable state, which means that the phenomena of ESD (solid line) and ESB (dotted line) are sensitive to the degree of entanglement of the initial state. The phenomena of ESD and ESB may simultaneously appear if we choose certain initial states. However, ESB ($C_{c_1c_3}$) disappears if the value of the parameter α is large enough.

Next, we turn to study ESB between the two optical fibers, f_1 and f_2. Tracing over the other degrees of freedom of the system, we deduce that the reduced density matrix of the two optical fibers is

$$\begin{aligned}\rho_{f_1f_2}(t) &= a_2(t)|00\rangle\langle 00| + b_2(t)|01\rangle\langle 01| + c_2(t)|10\rangle\langle 10| \\ &\quad + d_2(t)|11\rangle\langle 11| + f_2(t)|00\rangle\langle 11| + f_2^*(t)|11\rangle\langle 00| \end{aligned} \tag{15}$$

with

$$\begin{aligned} a_2(t) &= |\alpha|^2|A_1^2(t)|^2 + |\alpha|^2|B_1^2(t)|^2 + |\alpha|^2|C_1^2(t)|^2 \\ &\quad + |\alpha|^2|E_1^2(t)|^2 + 2|\alpha|^2|A_1(t)B_1(t)|^2 \\ &\quad + 2|\alpha|^2|A_1(t)C_1(t)|^2 + 2|\alpha|^2|A_1(t)E_1(t)|^2 \\ &\quad + 2|\alpha|^2|B_1(t)C_1(t)|^2 + 2|\alpha|^2|B_1(t)E_1(t)|^2 \\ &\quad + 2|\alpha|^2|C_1(t)E_1(t)|^2 + |\beta|^2 \\ b_2(t) = c_2(t) &= |\alpha|^2|A_1(t)D_1(t)|^2 + |\alpha|^2|B_1(t)D_1(t)|^2 \\ &\quad + |\alpha|^2|C_1(t)D_1(t)|^2 + |\alpha|^2|E_1(t)D_1(t)|^2 \\ d_2(t) &= |\alpha|^2|D_1^2(t)|^2 \\ f_2(t) &= \beta\alpha^* D_1^{*2}(t) \end{aligned} \tag{16}$$

Inserting (15) into (8), we find that the concurrence of two optical fibers is

$$C_{f_1f_2}(t) = 2\max\left\{0, |f_2(t)| - \sqrt{b_2(t)c_2(t)}\right\} \tag{17}$$

In Fig. 4 we plot the concurrence, $C_{f_1f_2}$, as a function of rescaled time, $\sqrt{N}gt$, with $|\alpha|^2 = 0.6$ and $|\beta|^2 = 0.4$ with two different values of the parameter r. From Fig. 4, we can see that the value of ESB ($C_{f_1f_2}$) decreases with the increase of the parameter r. It is worth noting that the ESB ($C_{f_1f_2}$) disappears if the parameter r is large enough.

4. Entanglement and entangled state transfer

In this section, we investigate the entanglement and entangled state transfer between the atoms. We first study the entanglement transfer between the atoms. Here, we adopt the concurrence as the method to quantify the degree of entanglement transfer. The concurrence of atomic traps 1 and 3 is introduced by (11). We now begin to calculate the concurrence between atomic traps 2 and 4. Tracing over the other degrees of freedom of the system, we obtain that the reduced density matrix of atomic traps 2 and 4 is

$$\begin{aligned}\rho_{24}(t) &= a_3(t)|1, N-1\rangle|1, N-1\rangle\langle 1, N-1|\langle 1, N-1| \\ &\quad + b_3(t)|1, N-1\rangle|0, N\rangle\langle 1, N-1|\langle 0, N| \\ &\quad + c_3(t)|0, N\rangle|1, N-1\rangle\langle 0, N|\langle 1, N-1| \\ &\quad + d_3(t)|0, N\rangle|0, N\rangle\langle 0, N|\langle 0, N| \end{aligned}$$

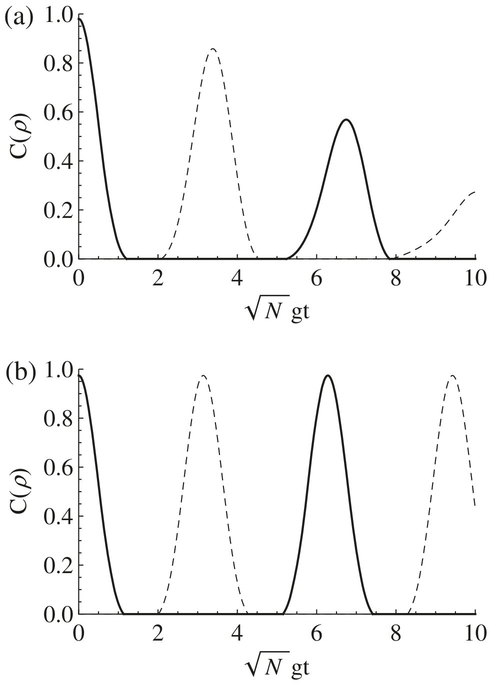

Fig. 5. The concurrences, C_{13} (solid line) and C_{24} (dotted line), are plotted as a function of rescaled time, $\sqrt{N}gt$, with $|\alpha|^2 = 0.6$ and $|\beta|^2 = 0.4$. (*a*) $r = 1$; (*b*) $r = \sqrt{1.5}$.

$$
\begin{aligned}
&+ f_3(t)|1, N-1\rangle|1, N-1\rangle\langle 0, N|\langle 0, N| \\
&\qquad + f_3^*(t)|0, N\rangle|0, N\rangle\langle 1, N-1|\langle 1, N-1|
\end{aligned} \tag{18}
$$

with

$$
\begin{aligned}
a_3(t) &= |\alpha|^2|A_1^2(t)|^2 \\
b_3(t) &= c_3(t) = |\alpha|^2|A_1(t)B_1(t)|^2 + |\alpha|^2|A_1(t)C_1(t)|^2 \\
&\qquad + |\alpha|^2|A_1(t)D_1(t)|^2 + |\alpha|^2|A_1(t)E_1(t)|^2 \\
d_3(t) &= |\alpha|^2|B_1^2(t)|^2 + |\alpha|^2|C_1^2(t)|^2 + |\alpha|^2|D_1^2(t)|^2 \\
&\quad + |\alpha|^2|E_1^2(t)|^2 + 2|\alpha|^2|B_1(t)C_1(t)|^2 \\
&\quad + 2|\alpha|^2|B_1(t)D_1(t)|^2 + 2|\alpha|^2|B_1(t)E_1(t)|^2 \\
&\quad + 2|\alpha|^2|C_1(t)D_1(t)|^2 + 2|\alpha|^2|C_1(t)E_1(t)|^2 \\
&\qquad\qquad + 2|\alpha|^2|D_1(t)E_1(t)|^2 + |\beta|^2 \\
f_3(t) &= \alpha\beta^* A_1^2(t)
\end{aligned} \tag{19}
$$

Inserting the above density matrix into (8), we find that the concurrence between atomic traps 2 and 4 is

$$
C_{24}(t) = 2\max\left\{0, |f_3(t)| - \sqrt{b_3(t)c_3(t)}\right\} \tag{20}
$$

In Fig. 5, we plot the simultaneous concurrences of atomic traps 1 and 3, C_{13} (solid line), and atomic traps 2 and 4, C_{24} (dotted line), as a function of rescaled time, $\sqrt{N}gt$, with $|\alpha|^2 = 0.6$ and $|\beta|^2 = 0.4$ with two different values of the parameter r. It is shown that the entanglement of the transferred state oscillates periodically in both case. Comparing Figs. 5*a* and 5*b*, it is not difficult to see that perfect entanglement transfer is implemented if we choose the value of the parameter r to be around $\sqrt{1.5}$.

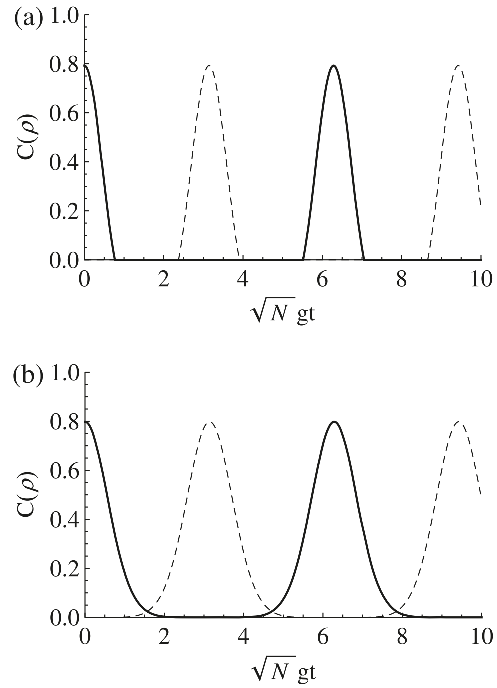

Fig. 6. The concurrences, C_{13} (solid line) and C_{24} (dotted line), as a function of rescaled time, $\sqrt{N}gt$, with $r = \sqrt{1.5}$. (*a*) $|\alpha|^2 = 0.8$ and $|\beta|^2 = 0.2$; (*b*) $|\alpha|^2 = 0.2$ and $|\beta|^2 = 0.8$.

To illustrate the influence of the initial states on the entanglement transfer, the concurrences, C_{13} (solid line) and C_{24} (dotted line), are displayed as a function of rescaled time, $\sqrt{N}gt$, for $r = \sqrt{1.5}$ with two different initial states in terms of α in Fig. 6. It is not difficult to see that the length of zero entanglement time interval is dependent on the coefficient α of the initial state. The larger the coefficient α of initial state, the longer the state stays in the separable state. This means that by tuning the coefficients of the initial states, it would be possible to improve the transferred entanglement. It is worth noting that for some initial states, the phenomenon of ESD may completely disappear.

Next, we investigate the entangled state transfer between atomic traps 1 and 3 and atomic traps 2 and 4. To quantify the degree of entangled state transfer, we adopt the fidelity, which is introduced by Nielsen and Paulina Marian [2, 23]

$$
F(\rho_1, \rho_2) = \langle \Psi_1|\rho_2|\Psi_1\rangle \tag{21}
$$

From (3), we can find the target state $|\varphi_p\rangle$ of the transmission is

$$
\begin{aligned}
|\varphi_p\rangle &= (\alpha|1, N-1\rangle_2|1, N-1\rangle_4 + \beta|0, N\rangle_2|0, N\rangle_4) \otimes |0, N\rangle_1 \\
&\qquad \otimes |0, N\rangle_3 \otimes |000\rangle_{c_1c_2f_1} \otimes |000\rangle_{c_3c_4f_2}
\end{aligned} \tag{22}
$$

Inserting (22) and (4) into (21), we can obtain the fidelity of entangled state transfer between atomic traps 1 and 3 and atomic traps 2 and 4 as follows

$$
F(t) = |\alpha|^4|A_1^2(t)|^2 + |\alpha\beta|^2(A_1^2(t) + A_1^{*2}(t)) + |\beta|^4 \tag{23}
$$

In Fig. 7, we plot the fidelity, $F(t)$, as a function of rescaled time, $\sqrt{N}gt$, for $|\alpha|^2 = 0.6$ and $|\beta|^2 = 0.4$ with three different values of the parameter r. We find that the perfect

Fig. 7. The fidelity of quantum entangled state transfer, $F(t)$, is plotted as a function of rescaled time, $\sqrt{N}gt$, for $|\alpha|^2 = 0.6$ and $|\beta|^2 = 0.4$ with $r = \sqrt{0.5}$ (dotted line), $r = 1$ (dashed line), $r = \sqrt{1.5}$ (solid line).

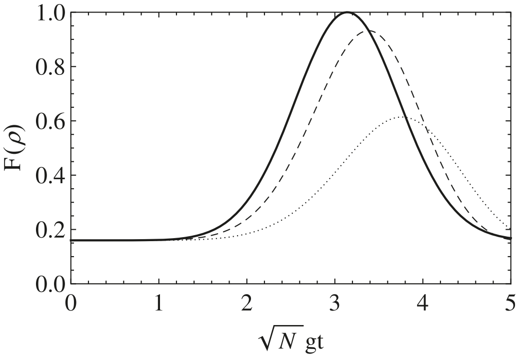

Fig. 8. The fidelity of atomic traps 1 and 3 is plotted as a function of rescaled time, $\sqrt{N}gt$, with $r = \sqrt{1.5}$ for $|\alpha|^2 = 0.6$ and $|\beta|^2 = 0.4$ (dotted line), $|\alpha|^2 = 0.8$ and $|\beta|^2 = 0.2$ (solid line).

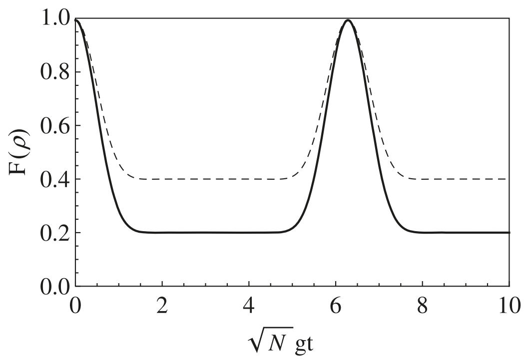

entangled state transfer can be implemented if we choose the value of the parameter r to be around $\sqrt{1.5}$. From Fig. 7, it is also obvious that the fidelity varies smoothly as a function of the rescaled time. This feature is useful for switching off the interaction between the atoms and the cavities fields using control pulses once the quantum entangled state transfer is achieved. It is worth noting that the different choices of α and β do not give qualitatively different results from the case treated here.

Furthermore, it is interesting to compare the fidelity dynamics with the entanglement dynamics between atomic traps 1 and 3. Using (3), (9), and (21), the fidelity of atomic traps 1 and 3 is shown as a function of rescaled time, $\sqrt{N}gt$, for $r = \sqrt{1.5}$ with two different initial entanglement degrees in Fig. 8. It is obvious that when the value of the state parameter, α, is increased, the fidelity decreases faster and the state stays in the separable state longer. It is worth pointing out that the different bipartite concurrences of the system and the fidelity of the entangled state transfer in the case of off-resonance are similar to the previous results, which are obtained in the resonance case.

5. Summary

In the present paper, we investigate multiatom entanglement dynamics, entanglement, and entangled state transfer of a system consisting of two identical subsystems (as shown in Fig. 1). Each subsystem contains multiple two-level atoms, which are trapped in two distant single-mode optical cavities that are connected by two optical fibers. It is shown that the phenomena of ESD and ESB may appear in this system, and the amount of entanglement of the atoms or the other bipartite partitions of the system is sensitive to the initial states and the parameter r. Particularly, we find that the concurrence C_{13} reaches a maximum if we choose the value of parameter r to be around $\sqrt{1.5}$, but the concurrences $C_{c_1c_3}$ and $C_{f_1f_2}$ become smaller when the value of parameter r increases. In addition, we also study the entanglement and entangled state transfer between the atoms and find that perfect entanglement and entangled state transfer can be achieved if we choose the value of parameter r to be around $\sqrt{1.5}$. It is worth noting that the fidelity varies smoothly as a function of the rescaled time, and we can make use of this feature to apply different methods (such as control pulses) to switch off the interaction between the atoms and the cavity fields when the entanglement and entangled state transfer are achieved. In that way, the perfect long-time transmission of entanglement and entangled state will be achieved. The approach presented in this paper may have potential applications in quantum information processing.

Acknowledgement

This project was supported by the National Natural Science Foundation of China (Grant No. 10774131).

References

1. A. Einstein, B. Podolsky, and N. Rosen. Phys. Rev. **47**, 777 (1935). doi:10.1103/PhysRev.47.777.
2. M.A. Nielsen and I.L. Chuang. Quantum computation and quantum information. Cambridge University Press, Cambridge. 2000.
3. C.H. Bennett, G. Brassard, C. Crépeau, R. Jozsa, A. Peres, and W.K. Wootters. Phys. Rev. Lett. **70**, 1895 (1993). doi:10.1103/PhysRevLett.70.1895. PMID:10053414.
4. S.L. Braunstein and H.J. Kimble. Phys. Rev. Lett. **80**, 869 (1998). doi:10.1103/PhysRevLett.80.869.
5. J.-W. Pan, D. Bouwmeester, H. Weinfurter, and A. Zeilinger. Phys. Rev. Lett. **80**, 3891 (1998). doi:10.1103/PhysRevLett.80.3891.
6. T. Yu and J.H. Eberly. Phys. Rev. Lett. **93**, 140404 (2004). doi:10.1103/PhysRevLett.93.140404. PMID:15524773.
7. B. Bellomo, R. Lo Franco, and G. Compagno. Phys. Rev. Lett. **99**, 160502 (2007). doi:10.1103/PhysRevLett.99.160502. PMID:17995229.
8. H.-T. Cui, K. Li, and X.-X. Yi. Phys. Lett. A, **365**, 44 (2007). doi:10.1016/j.physleta.2006.12.049.
9. M. Yönaçc, T. Yu, and J.H. Eberly. J. Phys. At. Mol. Opt. Phys. **39**, S621 (2006). doi:10.1088/0953-4075/39/15/S09.
10. J.-S. Zhang and J.-B. Xu. Opt. Commun. **05**, 78 (2009).
11. T. Yu and J.H. Eberly. Science, **323**, 598 (2009). doi:10.1126/science.1167343. PMID:19179521.
12. M.P. Almeida, F. de Melo, M. Hor-Meyll, A. Salles, S.P. Walborn, P.H.S. Ribeiro, and L. Davidovich. Science, **316**, 579 (2007). doi:10.1126/science.1139892. PMID:17463284.
13. J. Laurat, K.S. Choi, H. Deng, C.W. Chou, and H.J. Kimble. Phys. Rev. Lett. **99**, 180504 (2007). doi:10.1103/PhysRevLett.99.180504. PMID:17995390.

14. C.E. López, G. Romero, F. Lastra, E. Solano, and J.C. Retamal. Phys. Rev. Lett. **101**, 080503 (2008). doi:10.1103/PhysRevLett.101.080503. PMID:18764597.
15. D.L. Moehring, P. Maunz, S. Olmschenk, K.C. Younge, D.N. Matsukevich, L.-M. Duan, and C. Monroe. Nature, **449**, 68 (2007). doi:10.1038/nature06118. PMID:17805290.
16. W. Rosenfeld, S. Berner, J. Volz, M. Weber, and H. Weinfurter. Phys. Rev. Lett. **98**, 050504 (2007). doi:10.1103/PhysRevLett.98.050504. PMID:17358837.
17. D.N. Matsukevich, T. Chanelière, S.D. Jenkins, S.-Y. Lan, T.A. B. Kennedy, and A. Kuzmich. Phys. Rev. Lett. **96**, 030405 (2006). doi:10.1103/PhysRevLett.96.030405. PMID: 16486672.
18. Z.-Q. Yin and F.-L. Li. Phys. Rev. A, **75**, 012324 (2007). doi:10.1103/PhysRevA.75.012324.
19. A. Serafini, S. Mancini, and S. Bose. Phys. Rev. Lett. **96**, 010503 (2006). doi:10.1103/PhysRevLett.96.010503. PMID: 16486430.
20. T. Pellizzari. Phys. Rev. Lett. **79**, 5242 (1997). doi:10.1103/PhysRevLett.79.5242.
21. W.K. Wootters. Phys. Rev. Lett. **80**, 2245 (1998). doi:10.1103/PhysRevLett.80.2245.
22. K.M. O'Connor and W.K. Wootters. Phys. Rev. A, **63**, 052302 (2001). doi:10.1103/PhysRevA.63.052302.
23. P. Marian and T.A. Marian. Phys. Rev. A, **76**, 054307 (2007). doi:10.1103/PhysRevA.76.054307.